

A Trimeric HIV-1 Fusion Peptide Construct Which Does Not Self-Associate in Aqueous Solution and Which Has 15-Fold Higher Membrane Fusion Rate

Rong Yang,[†] Mary Prorok,[‡] Francis J. Castellino,[‡] and David P. Weliky^{*†}

Department of Chemistry, Michigan State University, East Lansing, Michigan 48824, and Department of Chemistry and Biochemistry and W. M. Keck Center for Transgene Research, University of Notre Dame, Notre Dame, Indiana 46556

Received July 21, 2004; E-mail: weliky@chemistry.msu.edu

Enveloped viruses such as HIV-1 are surrounded by a membrane and enter into host cells via fusion of the viral membrane with the target cell membrane.^{1,2} Fusion is mediated by envelope proteins in the viral membrane which contain apolar fusion peptide (FP) domains that interact with the target cell membrane and play a key role in membrane fusion.³ For the HIV-1 virus, the FP is the ~20 N-terminal amino acids of the gp41 envelope protein, and peptides composed of the FP sequence induce fusion between large unilamellar vesicles (LUVs) or between red blood cells.⁴ There are similar mutation/fusion activity relationships for peptide-induced fusion and virus-induced fusion which suggests that the peptide by itself is a useful model system to understand some aspects of viral/target cell fusion.^{3,5} There are also high-resolution structures of the gp41 "soluble ectodomain" which begins ~10 residues C-terminal of the FP.² Although the apolar FP is not part of the soluble ectodomain, the structures show trimeric oligomerization with the three N-termini in close proximity. These data suggest that during viral/target cell fusion, gp41 is trimeric with the C-termini of three FPs close together. In an effort to mimic the biologically relevant topology in a peptide model system, we have synthesized and functionally characterized a fusion peptide trimer (FPtr) whose three FP strands are chemically bonded at their C-termini. To assess the significance of the oligomeric topology and of trimerization, comparative measurements were made for monomeric (FPmn) and cross-linked dimeric (FPdm) peptides. The amino acid sequences of all of the peptides are displayed in Figure 1A. In addition to the native FP sequence, the peptides contain lysines in their C-terminal regions to improve aqueous solubilities and tryptophans as 280 nm chromophores.⁶ One strand of FPtr also has a C-terminal β -alanine because it was included in the commercial low-substitution resin used in the synthesis.

FPdm was synthesized by cross-linking two monocysteine peptides.⁷ Trimer synthesis had previously been attempted by cross-linking dicysteine and monocysteine peptides in 1:4 ratio, but as would be expected from statistics, this approach gave very high yield of dimer and very low (~1%) yield of trimer. In the present study, the trimer was synthesized with a lysine side chain scaffold and gave ~6% (0.6 μ mol) purified yield. Fluorenylmethoxycarbonyl (Fmoc)-based solid-phase methods were used, and the trimer backbone was initially formed with two sequential couplings of *N*- α -Fmoc-*N*- ϵ -4-methyltrityl-L-lysine (Fmoc-Lys(Mtt)) followed by a coupling with *N*- α -Fmoc-*N*- ϵ -*tert*-butoxycarbonyl-L-lysine. Prior to the second and third couplings, the Mtt group on the lysine side chain was removed with 1% trifluoroacetic acid (TFA) in dichloromethane.⁸ The rest of the trimer was then synthesized using standard Fmoc peptide chemistry followed by cleavage from the resin with 80% TFA and purification with reversed-phase HPLC.

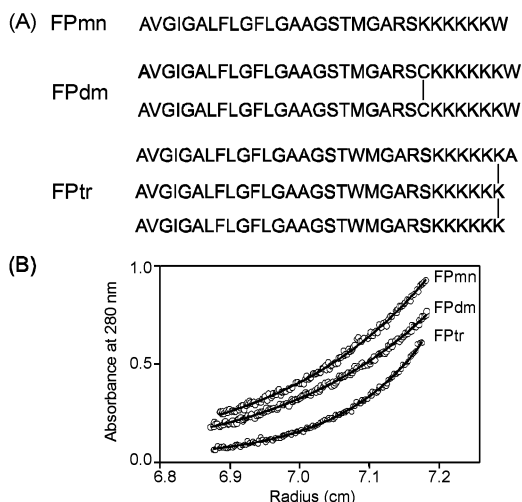


Figure 1. (A) FP constructs and (B) sedimentation equilibrium analytical ultracentrifugation data and fitting. The buffer solution was 5 mM HEPES pH 7 and the FPmn, FPdm, and FPtr concentrations were ~100, 40, and 25 μ M, respectively. The fitted FPmn, FPdm, and FPtr masses in solution are 3000, 5700, and 11000 g/mol, respectively, and are close to the actual nonassociated peptide masses of 3080, 6364, and 9274 g/mol.

One goal of the present study is correlation of the different numbers of strands in FPmn, FPdm, and FPtr with their respective fusion activities. In fusion assays, FPs bind to membranes from aqueous solution, and the correlation of fusogenicity with numbers of strands could be confounded by prior self-association of FPs in aqueous solution, as has been commonly observed with other FP constructs.^{7,9} Figure 1B displays analytical ultracentrifugation data for the present study's constructs at concentrations comparable to those of functional assay stock solutions. The fitted masses in solution are close to the masses of nonself-associated FPs. To our knowledge, this is the first demonstration of a homologous series of nonself-associated FPmn, FPdm, and FPtr constructs.

The fusion activities of the different constructs were assessed using a fluorescence assay which probed FP-induced mixing of lipids between different LUVs.¹⁰ Lipid mixing represents one of the steps in viral/target cell membrane fusion. Mixing was probed with LUVs of two different lipid compositions: (1) PC/PG-POPC and POPG in a 4:1 mol ratio; and (2) LM3-POPC, POPE, POPS, PI, sphingomyelin, and cholesterol in a 10:5:2:2:1:10 mol ratio. PC/PG has been a common composition used in studies of FPs, and LM3 reflects the approximate lipid headgroup and cholesterol composition of membranes of host cells of the virus.¹¹ In addition, solid-state NMR structural measurements are consistent with predominant helical conformation for PC/PG-associated FPs and with predominant β -strand conformation for LM3-associated FPs. For example, the Phe-8 ¹³C carbonyl shift for FPtr is ~178 ppm in

[†] Michigan State University.

[‡] University of Notre Dame.

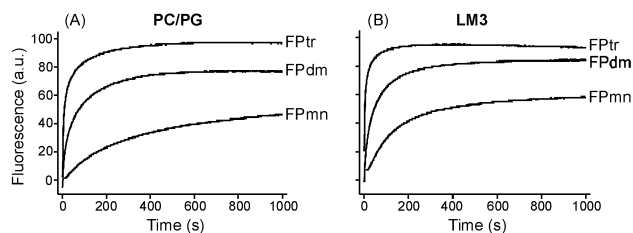


Figure 2. Stopped-flow fluorescence data for FP-induced lipid mixing in (A) PC/PG and (B) LM3 vesicles at 37 °C and [total lipid] = 150 μ M, [FPmn] = 1.5 μ M, FPdm = 0.75 μ M, and FPTr = 0.50 μ M.

Table 1. Kinetic Parameters of FP-Induced Vesicle Fusion^a

	PC/PG			LM3		
	FPmn	FPdm	FPTr	FPmn	FPdm	FPTr
k (10^{-3} s $^{-1}$)	13	63	190	11	76	430
E_a (kJ/mol)	54(7)	48(3)	27(1)	n.d.	n.d.	33(2)
$\ln A$	17(3)	16(1)	9(1)	n.d.	n.d.	12(1)
ΔS^\ddagger (J/mol-K)	-120	-130	-190	n.d.	n.d.	-160

^a The listed k and ΔS^\ddagger values are at 37 °C. Each k value has $\pm 20\%$ uncertainty, and the fitting uncertainties in E_a and $\ln A$ are given in parentheses. n.d. \equiv not determined because of significant uncertainties in Arrhenius fitting parameters (see Supporting Information).

PC/PG and ~ 173 ppm in LM3, which are consistent with helical and β -strand conformations, respectively.¹² The NMR samples were prepared under conditions similar to the fusion assays, and there was approximately quantitative binding of the FPs to membranes in these samples.

Figure 2 displays stopped-flow fluorescence data for FP-induced lipid mixing. In the assays, [FPmn] = 2[FPdm] = 3[FPTr], and the strand concentration was constant among the different constructs. The long-time changes in fluorescence are ordered $\Delta F_{mn} < \Delta F_{dm} < \Delta F_{tr}$, which suggests that the oligomeric constructs induce more vesicle fusion than FPmn. Because an increased fusion rate is likely the most important FP effect in viral/target cell fusion, the kinetics of the stopped-flow fluorescence data were analyzed to determine the variation of fusion rate with FP construct. In a single data set, the initial increase in fluorescence could be modeled by a dominant fast exponential buildup, while at longer time, there was an additional contribution from a slower buildup. The fast component likely represents the lipid mixing induced by initial interaction of FPs with membranes, and the values of its rate constant are listed in Table 1. For both PC/PG and LM3 vesicles, $k_{tr} > k_{dm} > k_{mn}$ with $k_{tr} \approx 15k_{mn}$ for PC/PG and $k_{tr} \approx 40k_{mn}$ for LM3. Thus, there is very significant correlation of the fusion rate with both the oligomeric topology enforced by C-terminal cross-linking and with the number of FP strands in the construct. Vesicle fusion does not appear to be diffusion-limited, as the k values are at most several percent of the vesicle collision rate.¹³

In an Arrhenius model, $k = A e^{-E_a/RT}$, and the variations in rate constants would have contributions from differences in activation energy E_a and differences in preexponential factor A . To quantify these contributions, assays and kinetic analyses were carried out over a temperature range of 25–40 °C. As displayed in Table 1, Arrhenius plots of the data yielded values of E_a and $\ln A$ for FP-induced lipid mixing in PC/PG and LM3. The values of E_a and $\ln A$ are similar for FPTr-induced fusion of either PC/PG or LM3 LUVs, and in PC/PG, $E_{a-tr} < E_{a-dm}$, E_{a-mn} , and $A_{tr} < A_{dm}$, A_{mn} . Thus, the changes in E_a and A appear to have competing effects on the magnitude of k . The entropy of activation ΔS^\ddagger at 37 °C was approximately calculated with the transition-state theory expression $\Delta S^\ddagger = R[\ln(Ah/k_B T) - 2]$ where R , h , and k_B are the standard

physical constants.¹⁴ It is not yet clear why $\Delta S^\ddagger < 0$ for all constructs and why $\Delta S_{tr}^\ddagger < \Delta S_{dm}^\ddagger$, ΔS_{mn}^\ddagger .

In summary, enforcement of the trimeric biological FP strand topology by cross-linking reduces E_a and increases the fusion rate by a factor of 15–40. The effect is observed both for PC/PG and for LM3 fusion in which the membrane-associated FPs have dominant helical and β -strand conformations, respectively. For FPdm or FPTr in either conformation, one reason for the fusogenic enhancement may be placement of the apolar N-terminal regions of strands on one end of the oligomer and placement of the more polar C-terminal regions of strands on the other end of the oligomer. FPTr likely has the largest apolar volume which may correlate with the greatest membrane disruption and fusion rate for this construct. Fusion may also be enhanced by the larger localized free energy released upon membrane binding of multiple FP strands in FPdm and FPTr. We note that enhanced fusion has also been observed with influenza protein constructs which likely contain FPs in the biologically relevant trimeric topology.¹⁵

Because it is possible to obtain FPTr in ~ 0.5 μ mol quantities and because it has negligible self-association in aqueous solution, it should be possible to study its structural and motional properties in aqueous, detergent, and membrane environments with a variety of biophysical methods. These studies should provide further insight into its enhanced fusion rate. The synthetic approach should also be applicable to fusion peptides from other viruses and perhaps to other membrane-associated peptides derived from proteins of known oligomeric stoichiometry.

Acknowledgment. This work was supported by NIH. We acknowledge assistance from Zhaoxiong Zheng, Michele Bodner, Rhonda Husain, Dr. Honggao Yan, and Dr. Ned Jackson.

Supporting Information Available: Detailed descriptions of the FPTr synthesis, analytical ultracentrifugation experiments, and lipid mixing assays and analyses including full chemical names of lipids; circular dichroism data and solid-state NMR spectra. This material is available free of charge via the Internet at <http://pubs.acs.org>.

References

- Hernandez, L. D.; Hoffman, L. R.; Wolfsberg, T. G.; White, J. M. *Annu. Rev. Cell Dev. Biol.* **1996**, *12*, 627–661.
- Eckert, D. M.; Kim, P. S. *Annu. Rev. Biochem.* **2001**, *70*, 777–810 and references therein.
- Durell, S. R.; Martin, I.; Ruysschaert, J.-M.; Shai, Y.; Blumenthal, R. *Mol. Membr. Biol.* **1997**, *14*, 97–112.
- (a) Freed, E. O.; Myers, D. J.; Risser, R. *Proc. Natl. Acad. Sci. U.S.A.* **1990**, *87*, 4650–4654. (b) Mobley, P. W.; Lee, H. F.; Curtain, C. C.; Kirkpatrick, A.; Waring, A. J.; Gordon, L. M. *Biochim. Biophys. Acta* **1995**, *1271*, 304–314. (c) Pereira, F. B.; Goñi, F. M.; Muga, A.; Nieva, J. L. *Biophys. J.* **1997**, *73*, 1977–1986.
- (a) Freed, E. O.; Delwart, E. L.; Buchschacher, G. L., Jr.; Panganiban, A. T. *Proc. Natl. Acad. Sci. U.S.A.* **1992**, *89*, 70–74. (b) Pereira, F. B.; Goñi, F. M.; Nieva, J. L. *FEBS Lett.* **1995**, *362*, 243–246. (c) Klinger, Y.; Aharoni, A.; Rapaport, D.; Jones, P.; Blumenthal, R.; Shai, Y. *J. Biol. Chem.* **1997**, *272*, 13496–13505.
- Han, X.; Tamm, L. K. *Proc. Natl. Acad. Sci. U.S.A.* **2000**, *97*, 13097–13102.
- Yang, R.; Yang, J.; Weliky, D. P. *Biochemistry* **2003**, *42*, 3527–3535.
- Aletras, A.; Barlos, K.; Gatos, D.; Koutsogianni, S.; Mamos, P. *Int. J. Pept. Protein Res.* **1995**, *45*, 488–496.
- Yang, J.; Prorok, M.; Castellino, F. J.; Weliky, D. P. *Biophys. J.* **2004**, *87*, 1951–1963.
- Struck, D. K.; Hoekstra, D.; Pagano, R. E. *Biochemistry* **1981**, *20*, 4093–4099.
- Aloia, R. C.; Tian, H.; Jensen, F. C. *Proc. Natl. Acad. Sci. U.S.A.* **1993**, *90*, 5181–5185.
- Zhang, H.; Neal, S.; Wishart, D. S. *J. Biomol. NMR* **2003**, *25*, 173–195.
- Steinfeld, J. I.; Francisco, J. S.; Hase, W. L. *Chemical Kinetics and Dynamics*; Prentice Hall: Upper Saddle River, NJ, 1999; p 131.
- McQuarrie, D. A.; Simon, J. D. *Physical Chemistry: A Molecular Approach*; University Science Books: Sausalito, CA, 1997; p 1168.
- (a) Epand, R. F.; Macosko, J. C.; Russell, C. J.; Shin, Y.-K.; Epand, R. M. *J. Mol. Biol.* **1999**, *286*, 489–503. (b) Lau, W. L.; Ege, D. S.; Lear, J. D.; Hammer, D. A.; DeGrado, W. F. *Biophys. J.* **2004**, *86*, 272–284.

JA0456120